APPLIED MECHANICS 2018
April 9 - 11, 2018, Myslovice, Czech republic

STUDY OF MIXED MODE CRACK PROPAGATION IN PIPE TYPE SPECIMEN

O. Slávik[1], P. Hutař[2], M. Berer[3], A. Gosch [4], F. Arbeiter[5], L. Náhlík[6]

Abstract: Fatigue specimens loaded in mixed mode are not used commonly. One of the reasons for this is that there are still not enough qualitative results, based on which it would be possible to tell in what way are the mode II and mode III affecting overall crack propagation. However, there is considerable number of parts loaded in mixed mode. Studying fatigue failure of roller bearing elements made of polymer material was a motivation to design an experimental specimen, on which the fracture behaviour of the material loaded in mixed mode could be observed. This work is dealing with FEM simulation of this specimen and calculation of fracture mechanics parameters.

Keywords: failure of polymer bearings, fracture mechanics, mixed mode, numerical modelling

1 Introduction

The fracture mechanics applications are traditionally concentrated on problems of crack growth under the mode I mechanism, resulting in a very good general knowledge about this phenomenon. On the other hand, the fatigue crack growth under the mixed mode loading conditions is still quite unexplored. There are very few studies such as [1] focused on this problem, even in the case of metals. However, a significant number of service failures occur due to the growth of cracks exposed to mixed mode loading [2].

An example of such mixed mode loaded component are roller bearing elements. Investigation of fatigue of roller bearing elements made of POM (Polyoxymethylene) and a general lack of knowledge about fatigue behaviour of materials in mixed modes caused a need to design a special specimen loaded under mixed mode conditions that could be used to observe the fatigue crack behaviour. Similar specimens that are dealing with mixed mode load can be found in [3] and [4]. The designed specimen has a shape of a pipe with two quarter-circumference notches, which have together four crack fronts (see Figure 1). As for the loading, the specimen is loaded by static/cyclic tension, which keeps the crack open and loaded in mode I, and by torque, responsible for mode II and III load. The goal of this work was to create a parametrical numerical model of the described specimen, in order to have a better look on the potential experimental results and possibly adjust some parameters if necessary. It will provide a better insight on how the specimen behaves under mixed mode conditions and what is to be expected.

2 Numerical model

[1] Ondrej Slávik, Institute of Physics of Materials, AS CR, and Institute of Solid Mechanics, Mechatronics and Biomechanics, BUT Faculty of Mechanical Engineering; Brno, Czech Republic, slavik@ipm.cz
[2] Pavel Hutař, Institute of Physics of Materials, AS CR, Brno; Czech Republic, hutar@ipm.cz
[3] Michael Berer; Polymer Competence Center Leoben GmbH, Roseggerstrasse 12, 8700 Leoben, Austria; michael.berer@pccl.at
[4] Anja Gosch; Material Science and Testing of Polymers, Montanuniversitaet Leoben, Otto Gloeckel-Straße 2, 8700 Leoben, Austria; anja.gosch@unileoben.ac.at
[5] Florian Arbeiter, Montanuniversität Leoben, Austria, florianarbeiter@uniloeben.ac.at
[6] Luboš Náhlík, CEITEC IPM, Brno, Czech Republic

Numerical model was created using software ANSYS. As was stated above, the designed fracture specimen has shape of a pipe. The whole specimen was modelled. Both geometry and boundary conditions, which were considered as tension and torque on the upper area of the specimen and fixed support on the bottom area, can be seen in the figure 1.

One of the most important points connected with the numerical modelling of cracks is the quality of the mesh, especially around the crack front, where the stress singularity occurs (see Figure 2). Fine mapped mesh was used in the close vicinity of all four crack fronts. Material model used in this work had material properties of POM. Specific values of Young's modulus and Poisson's ratio were 3600 MPa and 0.45 respectively. These values were taken from [5].

The aim of the calculation was to obtain the stress intensity factors (SIFs) for all modes of load (K_I, K_{II} and K_{III}). There are several possibilities of SIFs calculation in a 3D numerical model. In this case, the SIFs were calculated with interaction integral method using *CINT* command [6]. Then values of the elastic J-integral can be decomposed to the stress intensity factors in the corresponding three loading modes.

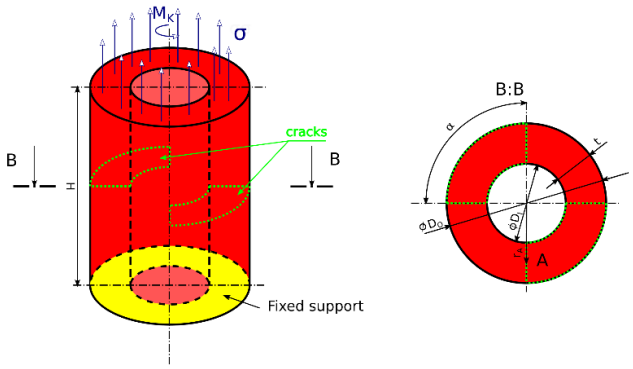

Figure 1: Geometry and boundary conditions of experimental specimens with notches

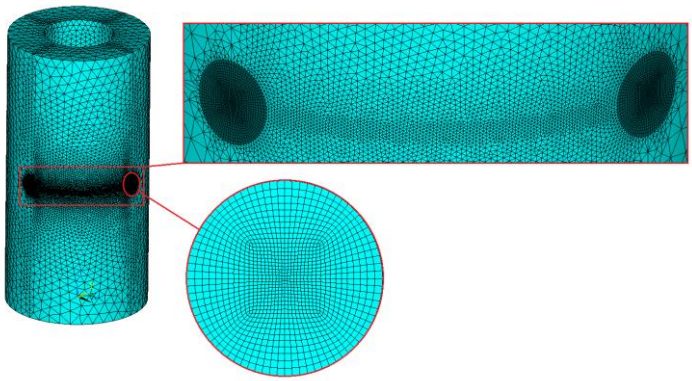

Figure 2: Numerical model of the test specimen with details of mesh refinement around the crack fronts (around $7x10^5$ elements)

3 Results

3.1 SIF Results

As stated the first evaluated parameters were SIFs. In the next three figures the dependency of SIFs on the normalized thickness can be seen. These values are computed for different input thicknesses *t* of the pipe and angles of the initial notch α (Figure 1). The purpose of the normalized thickness is to be able to compare dependencies of the SIFs on the radial distance from the middle of the pipe since these values would differ for cases with different thicknesses. The normalized pipe's wall thickness is therefore values from 0 to 1 (0 belongs to the inner diameter, 1 to the outer diameter).

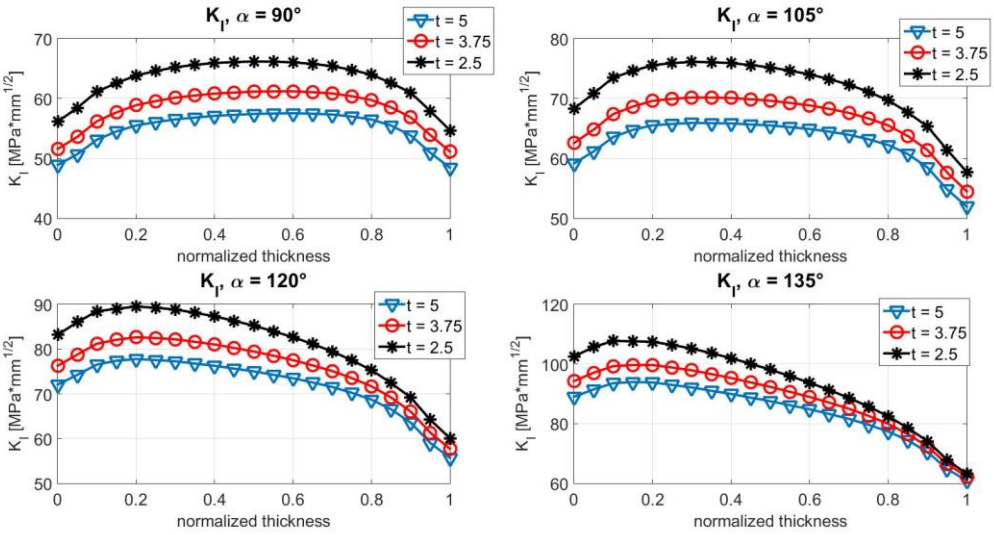

Figure 3: Dependency of the SIF K_I on the normalized thickness

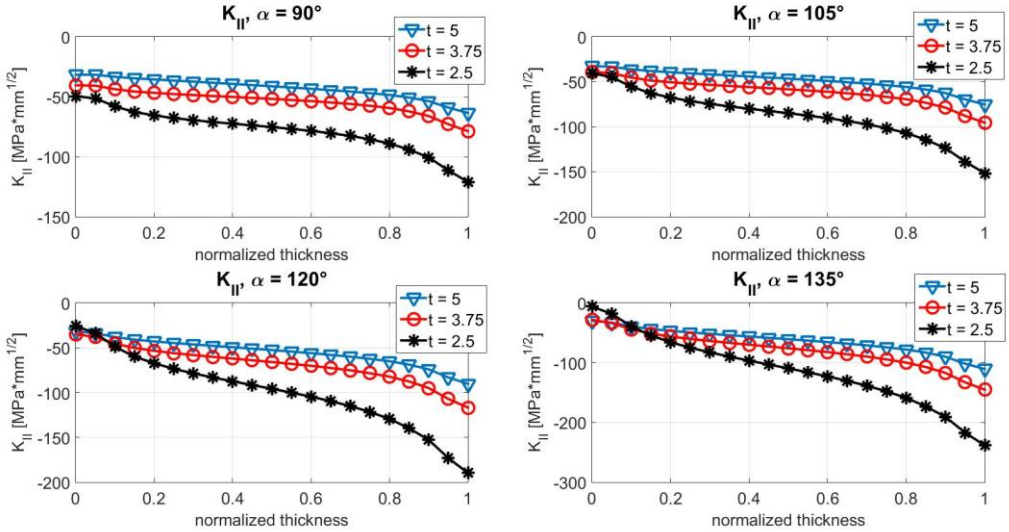

Figure 4: Dependency of the SIF K_{II} on the normalized thickness

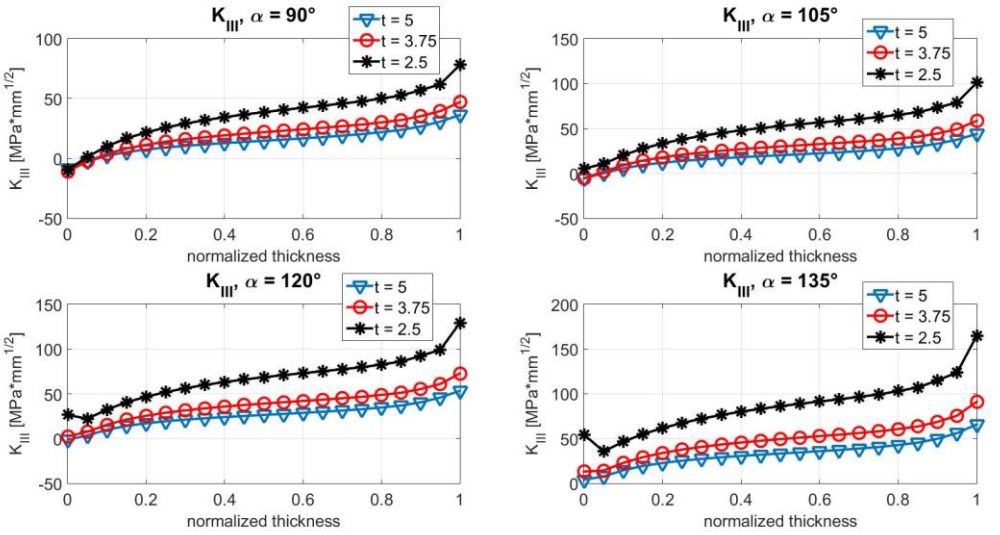

Figure 5: Dependency of the SIF K_{III} on the normalized thickness

3.2 SIF normalization

From figures 3, 4 and 5 it is evident, that no matter the thickness of the pipe or the angle of the initial notch, the graphs of function for given SIF show significant amount of similarity. Therefore it is possible to assume, that such functions could be normalized. In this work a normalization of all three SIFs was made with an output value of SIF in the middle of the pipe wall. These normalized values are also compared with computed values in tables 1, 2 and 3.

K_I normalization:

$$K_I^A = \sigma \cdot \sqrt{a} \cdot (1{,}0657 \cdot 10^{-4} \cdot \alpha^2 - 0{,}015 \cdot \alpha + 2{,}1582) \cdot (0{,}0054 \cdot t^2 - 0{,}0625 \cdot t + 1{,}774), \quad (1)$$

where

$$a = \pi \cdot r \cdot \frac{\alpha}{180}, \quad (2)$$

$$r = \frac{D_O + D_I}{4}, \quad (3)$$

$$t = \frac{D_O - D_I}{2}, \quad (4)$$

K_{II} normalization:

$$K_{II}^A = \tau_A \cdot \sqrt{a} \cdot (-9{,}3994 \cdot 10^{-5} \cdot \alpha^2 + 0{,}0142 \cdot \alpha - 2{,}0903) \cdot (0{,}0138 \cdot t^2 - 0{,}1248 \cdot t + 1{,}2789), \quad (5)$$

where a, r and t are taken from equations (2), (3) and (4) respectively,

$$\tau_A = \frac{D_O + D_I}{2 \cdot D_O} \cdot \tau_{max}, \quad (6)$$

$$\tau_{max} = \frac{M_k}{W_k}, \quad (7)$$

$$W_k = \frac{\pi}{16} \cdot D_o^3 \cdot \left(1 - \left(\frac{D_I}{D_o}\right)^4\right), \quad (8)$$

K_{III} normalization:

$$K_{III}^A = \tau_A \cdot \sqrt{a} \cdot (1{,}2904 \cdot 10^{-5} \cdot \alpha^2 + 0{,}0076 \cdot \alpha - 0{,}2301) \cdot (0{,}0408 \cdot t^2 - 0{,}5083 \cdot t + 2{,}5221), \quad (9)$$

where *a, r, t,* τ_A, τ_{max} and W_k are taken from equations (2), (3), (4), (6), (7) and (8) respectively.

t = 5	α [°]	K_I normalized [MPa*mm^2]	K_I J-int [MPa*mm^2]	(K_I normalized - K_I J-int/K_I normalized)*100 [%]
	90	57.4901712	57.436	0.094226882
	105	65.3329524	65.508	-0.267931542
	120	75.2044146	75.017	0.249206861
	135	87.4679598	87.534	-0.075502201
t = 3.75	α [°]	K_I normalized [MPa*mm^2]	K_I J-int [MPa*mm^2]	(K_I normalized - K_I J-int/K_I normalized)*100 [%]
	90	60.97262715	61.165	-0.315506915
	105	69.29048331	69.645	-0.511638355
	120	79.75990736	79.465	0.369743859
	135	92.76631443	92.342	0.457401411
t = 2.5	α [°]	K_I normalized [MPa*mm^2]	K_I J-int [MPa*mm^2]	(K_I normalized - K_I J-int/K_I normalized)*100 [%]
	90	65.50233178	66.198	-1.06205107
	105	74.43812806	75.202	-1.02618371
	120	85.68533389	85.233	0.527901179
	135	99.65799722	98.103	1.560333601

Table 1: Comparison of normalized and computed values of SIF K_I

t = 5	α [°]	K_{II} normalized [MPa*mm^2]	K_{II} J-int [MPa*mm^2]	(K_{II} normalized - K_{II} J-int/K_{II} normalized)*100 [%]
	90	-41.26406566	-41.228	0.087402105
	105	-46.32441487	-46.441	-0.251671028
	120	-52.67879425	-52.554	0.236896553
	135	-60.58000218	-60.624	-0.072627629
t = 3.75	α [°]	K_{II} normalized [MPa*mm^2]	K_{II} J-int [MPa*mm^2]	(K_{II} normalized - K_{II} J-int/K_{II} normalized)*100 [%]
	90	-51.73181972	-51.737	-0.010013712
	105	-58.07586432	-58.305	-0.394545443
	120	-66.04220509	-65.887	0.235008947
	135	-75.9477696	-75.819	0.169550208
t = 2.5	α [°]	K_{II} normalized [MPa*mm^2]	K_{II} J-int [MPa*mm^2]	(K_{II} normalized - K_{II} J-int/K_{II} normalized)*100 [%]
	90	-75.1031977	-75.226	-0.163511364
	105	-84.3133519	-84.917	-0.715957868
	120	-95.8787225	-95.735	0.149900311
	135	-110.2594184	-109.455	0.72956892

Table 2: Comparison of normalized and computed values of SIF K_{II}

t = 5	α [°]	K_{III} normalized [MPa*mm^2]	K_{III} J-int [MPa*mm^2]	(K_{III} normalized - K_{III} J-int/K_{III} normalized)*100 [%]
	90	14.75039776	14.757	-0.04475971
	105	20.24962329	20.228	0.106783679
	120	26.43904598	26.462	-0.086818623
	135	33.31125941	33.303	0.024794654
t = 3.75	α [°]	K_{III} normalized [MPa*mm^2]	K_{III} J-int [MPa*mm^2]	(K_{III} normalized - K_{III} J-int/K_{III} normalized)*100 [%]
	90	21.8856755	21.948	-0.28477301
	105	30.04506668	30.003	0.140011949
	120	39.22852727	39.171	0.146646532
	135	49.4250681	49.426	-0.001885472
t = 2.5	α [°]	K_{III} normalized [MPa*mm^2]	K_{III} J-int [MPa*mm^2]	(K_{III} normalized - K_{III} J-int/K_{III} normalized)*100 [%]
	90	38.39680106	38.704	-0.800063877
	105	52.71185019	52.73	-0.034432125
	120	68.82355345	68.618	0.298667306
	135	86.71263116	86.248	0.535828696

Table 3: Comparison of normalized and computed values of SIF K_{III}

3.3 Crack front propagation

Since this work is dealing with mixed mode loading conditions, it is proper to consider a change of crack growth trajectory. There are multiple articles about determining the angle of crack tip deflection under mixed mode conditions, such as [8] and [9] for example. Work [9] uses the criterion by Richard for evaluating the crack kinking angle (caused by mode II) and crack twisting angle (caused by mode III). Paper [8] uses the maximum tangential stress (MTS) criterion, which was formed by Sih and Erdogan in [7]. According to MTS criterion crack growth is initiating radially from the crack tip in direction of maximum tangential stress. In this work the angle of deflection of crack front (crack kinking) is calculated from evaluated values of SIFs K_I and K_{II} using following equation:

$$\beta = arccos\left(\frac{3\cdot K_{II}^2 + K_I\cdot\sqrt{K_I^2+8\cdot K_{II}^2}}{K_I^2+9\cdot K_{II}^2}\right), \tag{10}$$

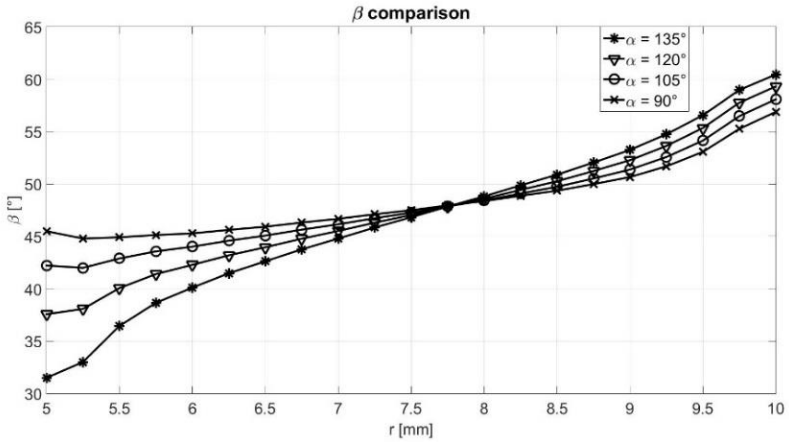

Figure 6: Dependence of the angle of the crack front deflection (crack kinking) along the crack front

It can be seen, that there is no SIF K_{III} present in equation (10). However, the angle β is calculated for multiple points of the crack front. It can be seen from the Figure 6, that for different points of the crack front the values of the angle β are also different, resulting in twisted crack front. This means that mode III effect is taken (at least partially) into account.

4 Conclusion

This paper presents results obtained by numerical model of cracked pipe specimen under mixed mode loading. The created model is parametric, which made it possible to obtain results of various combinations of input data. The model provided useful results in the form of SIFs, which refer to fatigue crack behaviour. From the similarities in SIFs graphs it was possible to create normalized shape functions for the given modes of load. Also the angle of deflection of the crack front was calculated. These results show the difference of the stress field close to inner diameter and close to outer diameter of the specimen. All the information obtained from the model can be used in the following works, which are going to be focused on carrying out actual experiments on the designed specimens and comparing experimental results of actually propagating cracks with the numerically calculated results.

Acknowledgement

This research has been supported by Polymer Competence Center Leoben GmbH (PCCL, Austria) and the Ministry of Education, Youth and Sports of the Czech Republic under the project m-IPMinfra (CZ.02.1.01/0.0/0.0/16_013/0001823) and the equipment and the base of research infrastructure IPMinfra were used during the research activities. Also, thanks are due to the specific research project FSI-S-17-4386 of the Faculty of Mechanical Engineering, BUT.

References

[1] H.A. Richard, B. Schramm, N.-H. Schirmeisen, Cracks on Mixed Mode loading – Theories, experiments, simulations, International Journal of Fatigue, Volume 62, 2014, Pages 93-103, ISSN 0142-1123, https://doi.org/10.1016/j.ijfatigue.2013.06.019.

[2] J. Qian, A. Fatemi, Mixed mode fatigue crack growth: A literature survey, Engineering Fracture Mechanics, Volume 55, Issue 6, 1996, Pages 969-990, ISSN 0013-7944, https://doi.org/10.1016/S0013-7944(96)00071-9.

[3] R. Citarella, R. Sepe, V. Giannella, I. Ishtyryakov, Multiaxial Fatigue Crack Propagation of an Edge Crack in a Cylindrical Specimen Undergoing Combined Tension-Torsion Loading, Procedia Structural Integrity, Volume 2, 2016, Pages 2706-2717, ISSN 2452-3216, ttps://doi.org/10.1016/j.prostr.2016.06.338.

[4] D. Rozumek, Z. Marciniak, G. Lesiuk, J.A.F.O. Correia, Mixed mode I/II/III fatigue crack growth in S355 steel, Procedia Structural Integrity, Volume 5, 2017, Pages 896-903, ISSN 2452-3216, https://doi.org/10.1016/j.prostr.2017.07.125.

[5] M. Berer, I. Mitev, G. Pinter, Finite element study of mode I crack opening effects in compression-loaded cracked cylinders, Engineering Fracture Mechanics, Volume 175, 2017, Pages 1-14, ISSN 0013-7944, https://doi.org/10.1016/j.engfracmech.2017.03.008.

[6] LAWRENCE, Kent L. ANSYS tutorial: release 11.0 : structural & thermal analysis using the ANSYS release 11.0 envirnoment. Mission: SDC Publications, 2007. ISBN 978-1-58503-400-0.

[7] F. Erdogan, G.C. Sih, **On the crack extension in plates under plane loading and transverse shear,** Journal of Basic Engineering, Transactions of ASME, 85 (1963), Pages 519-525

[8] M.R. Ayatollahi, M.R.M. Aliha, Mixed mode fracture in soda lime glass analysed by using the generalized MTS criterion, International Journal of Solids and Structures, Volume 46, Issue 2, 2009, Pages 311-321, ISSN 0020-7683, https://doi.org/10.1016/j.ijsolstr.2008.08.035.

[9] Richard, H.A., Eberlein, A., Kullmer, G., Concepts and experimental results for stable and unstable crack growth under 3D-mixed-mode-loadings, Engineering Fracture Mechanics (2016), doi: http://dx.doi.org/10.1016/j.engfracmech.2016.12.005